

Raman spectra evaluation of the carbon layers with Voigt profile

M. Gołabczak*, A. Konstantynowicz

Department of Production Engineering, Technical University of Lodz,
ul. Stefanowskiego 1/15, 90-924 Łódź, Poland

* Corresponding author: E-mail address: marcing@p.lodz.pl

Received 17.09.2009; published in revised form 01.12.2009

Materials

ABSTRACT

Purpose: Recent use of Raman spectroscopy as the valuable tool for investigations of the content and state of different material samples is rapidly growing especially in the area of the DLC (Diamond-Like Carbon) layers investigation. Not only qualitative analysis but also quantitative is in the scope of this method which in turn demands use of precise mathematical tools for describing spectrograms.

Design/methodology/approach: So-called Voigt profile establish basis for the relatively most precise shape-functions used for describing spectrogram shape. Voigt profile is the convolution of the very well known distribution functions: Gaussian distribution and Cauchy distribution (Lorentz distribution). Gaussian distribution is traditionally recognized as a tool for modeling multi-causal phenomena due to the Central Limit Theorem results. Cauchy distribution is recognized as modeling influence of the Fabry-Pérot interferometer (etalon) used for detection of the Raman spectrum.

Findings: We present successful decomposition of the Raman spectra into elements: base function, peaks' determination and etalon influence on spectral peaks' shapes. Thorough numerical simulation of the Fabry-Pérot interferometer has been performed and identification of its accuracy parameter has been done when matching Voigt profile based function to the experimental data.

Research limitations/implications: Good computational tools for generation of the Voigt profile, being not an analytical function itself and good understanding of mutual relationships between the Voigt profile and the Fabry-Pérot interferometer is of main interest for not only practical but also precise use this tool for quantitative analysis of Raman spectra.

Practical implications: The main goal of our work has been the thorough preparation for future works with spectrum deconvolution allowing better resolution in determining Raman spectrum components.

Originality/value: So far no proper attention has been paid to precise, quantitative analysis of the Raman spectra of the DLC layers.

Keywords: Nanomaterials; Raman spectra; Fabry-Pérot interferometer; Voigt profile

Reference to this paper should be given in the following way:

M. Gołabczaka, A. Konstantynowicz, Raman spectra evaluation of the carbon layers with Voigt profile, Journal of Achievements in Materials and Manufacturing Engineering 37/2 (2009) 270-276.

1. The DLC layer on the light alloy

In this paper we have been concerned with investigation of the thin DLC (Diamond-Like Carbon) layers imposed on the plates made of the

light alloys with plasma arc deposition method (PACVD). A sample layer prepared for different investigations is presented on the Fig. 1.

These layers have been investigated thoroughly with using different methods [6]. A few of this methods have been of mechanical type,

related with mechanical properties of the layer: nano-indentation and profile cut for measurement of the layer thickness [9], and scratching and friction tests for measurement usability merit of the layer. Also Raman spectrum investigation has been carried out for determining both layer composition and quantitative determination of the diamond-like structure participation in the layer.

Examination of the layer imposing procedure shows [5], that different carbon allotropes or compounds could be expected in the layer, not only diamond-like. Although efforts have been made to enhance content of the diamond-like structures is not possible to obtain a pure one. In our further works related with optimization of the layer content, especially assuring proper balance between diamond and graphite structures, we will need especially precise tools for quantitative examination of the layer, presumably more precise than tools based on the standard Raman spectrum profile matching for recognition purpose only.

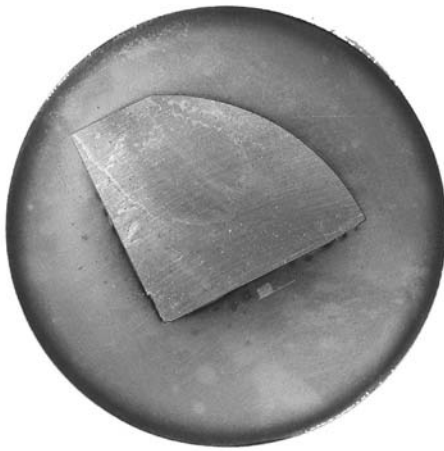


Fig. 1. Sample with DLC thin layer on the plate made of the light alloy, prepared for investigations

2. The Voigt profile basics

In the paper [6] we have examined use of different functions modeling shapes of the Raman spectrogram for different purposes. Here we like to deal in details with Voigt profile use and computational problems. Voigt profile is a specific convolution function, with two parameters, which covers features of the Raman spectrum generated by the investigated material features as well as the influence of the Fabry-Pérot interferometer used as the detector:

$$V(x, \sigma, \gamma) = \int_{-\infty}^{+\infty} G(t, \sigma) C(x-t, \gamma) dt \quad (1)$$

where: $G(x, \sigma)$ - central Gaussian (with zero mean value) distribution modeling features of the investigated material, given as the probability distribution function with one parameter σ determining its width:

$$G(x, \sigma) = \frac{1}{\sigma\sqrt{2\pi}} e^{-\frac{x^2}{2\sigma^2}} \quad (2)$$

$C(x, \gamma)$ - central Cauchy distribution modeling influence of the Fabry-Pérot

interferometer, called also “Lorentz distribution”, given as the probability distribution function with one parameter γ determining its width:

$$C(x, \gamma) = \frac{\gamma}{\pi(x^2 + \gamma^2)} \quad (3)$$

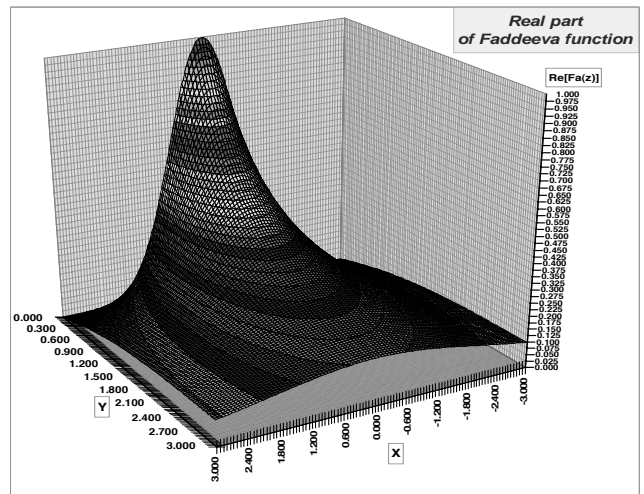
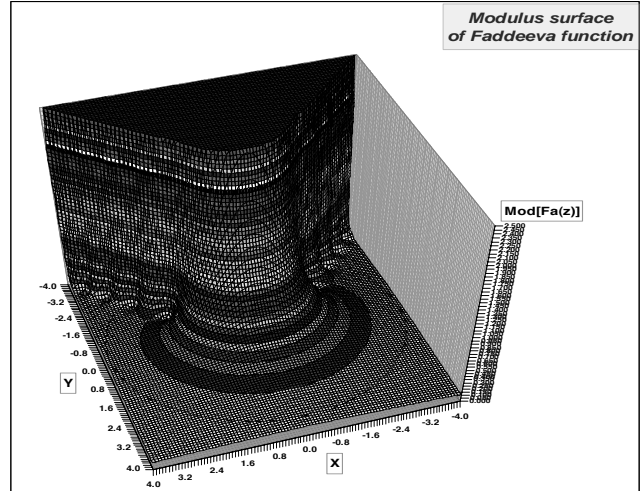


Fig. 2. Complex error function (Faddeeva function): modulus surface and real part surface

In closed form, after performing integration in convolution, Voigt profile can be expressed as:

$$V(x, \sigma, \gamma) = \frac{\text{Re}[F(z)]}{\sigma\sqrt{2\pi}} \quad (4)$$

where complex z variable is of the form:

$$z = \frac{x + j\gamma}{\sigma\sqrt{2}} \quad (5)$$

where in turn $F(z)$ is complex complementary error function called also Faddeeva function.

$$F(z) = e^{-z^2} \operatorname{erfc}(-jz) \tag{6}$$

where in turn:

$$\operatorname{erfc}(z) = 1 - \operatorname{erf}(z) \tag{7}$$

is the complementary error function of the complex variable expressed as (non-analytical!) integral:

$$\operatorname{erfc}(x) = \frac{2}{\sqrt{\pi}} \int_x^\infty e^{-t^2} dt \tag{8}$$

Effective computation of the *erfc* function i.e. fast and precise even for relatively big $|z|$, and the following computation Faddeeva function, establish a real problem. A number of methods is known, sometimes assuming very specific use in spectrum recognition, eq. [3]. They are all based on different approximations of the $F(z)$ function (power series expansions) easy (relatively!) for computation [2, 3, 8]. Sometimes these approximations are very specific and not usable beside rare programmatic environments or operating systems.

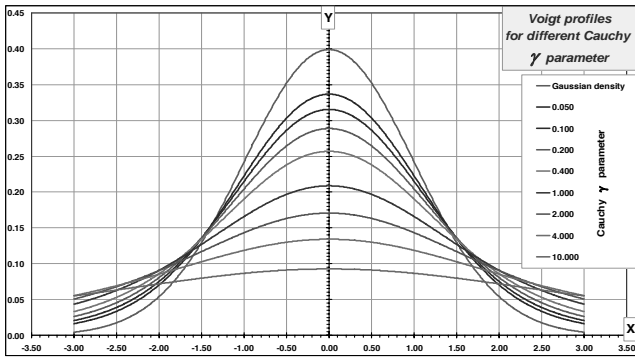


Fig. 3. Comparison of the Voigt profiles made of the normalized Gaussian density and the Cauchy densities of different width parameters γ

A universal and effective computation of the complex error function at the given point can be also performed traditionally by expansion in the Taylor power series [1], which seems to be more practical than basing upon the very special functions one can meet only in a few types of processors or programming languages:

$$\operatorname{erf}(z) = \frac{2}{\sqrt{\pi}} \sum_{n=0}^\infty \frac{(-1)^n z^{2n+1}}{n!(2n+1)} \tag{9}$$

from (6), (7) and (9) we obtain:

$$F(z) = e^{-z^2} \left(1 - \frac{2}{\sqrt{\pi}} \sum_{n=0}^\infty \frac{(-1)^n z^{2n+1}}{n!(2n+1)} \right) \tag{10}$$

Computing of the series (10) can be speed up with using two goals:

- iteratively counting each next summand from previous – it is so called conversion into multiplicative form of the (9) expression;
- performing full complex multiplication in algebraic form, not passing to trigonometrical functions which computation is the most long-lasting elementary operation.

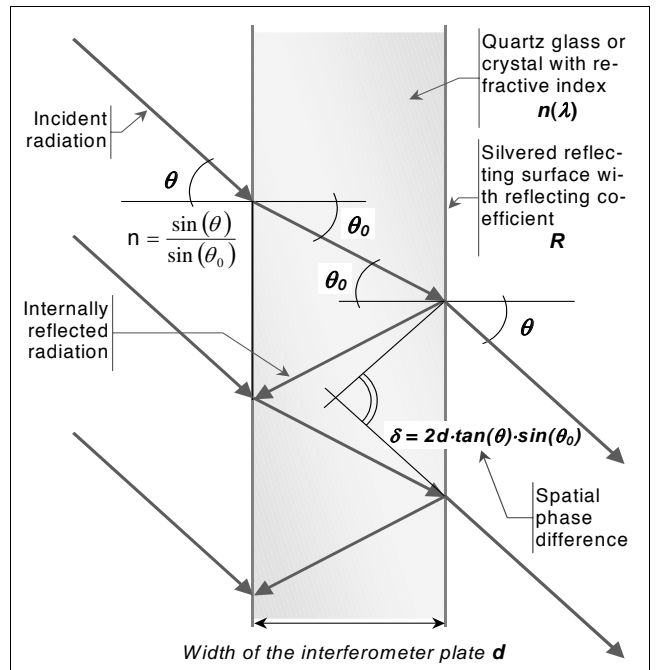


Fig. 4. Schematic diagram of the simply Fabry-Pérot interferometer and subsequent reflections of the interfering light beams

Preserving of the about 30 terms in power series allows to compute complex error function with relative error less than 10^{-10} in the neighborhood of center which is enough for most of the purposes. Increasing the number of terms to about 250 allows to compute function with the precision of 10^{-15} even at the radius of $|z|$ at the level of 5. This has been computationally proven in our practice.

Plots of the described functions are depicted on the Fig. 2. and on the Fig. 3.

3. The Fabry-Pérot interferometer

The Fabry-Pérot interferometer was developed in 1899 as a device for the very precise measurement of the length with using visible light wave as a “ruler”. This is also the origin of its other name – an “etalon”. Because of its excellent abilities in electromagnetic waves filtering in very narrow bands it has soon become a valuable tool in spectrometry. It is comprised of the two parallel surfaces reflecting light or electromagnetic wave from the other range eq. infrared or ultraviolet. Light is reflected and transmitted through the interferometer plate and reflected internally many times. Incident beam interfere with internally reflected, which gives an effect of selective passing the electromagnetic wave through the plate in the very narrow bands – transmission windows. This process is depicted schematically on the Fig. 4. where one of the possible configurations is considered. More sophisticated constructions based on two wedged plates are in use as well as the three plates assemblies, however this simply scheme covers the scope of our investigations with sufficient precision [4, 7].

Preserving of the parallelness of the surfaces is essential for the precision of the interferometer both in making the transmission window as narrow as possible and assuring that it is set in the

prescribed point of the whole spectrum [7]. This precision is in the scope of our special attention and will be practically identified from Raman spectrograms. We have been considered also with the tuning mechanisms of the Fabry-Pérot interferometers, but at this stage of investigations we have found them neglectable [11].

Spatial phase difference between two consecutive beams internally reflected – see the Fig. 4. is given by the equation, setting up base relationship in the Fabry-Pérot interferometer analysis:

$$\delta = \frac{2\pi}{\lambda} \cdot 2 \cdot n(\lambda) \cdot d \cdot \cos(\theta) \quad (11)$$

where: λ - wavelength of the incident electromagnetic radiation, [m];

$n(\lambda)$ - refraction index of the material between reflecting surfaces, variable along the wavelength of the radiation, [-];

d - distance between reflecting surfaces, normally is the thickness of the plate, eq. made of quartz crystal or quartz glass, which surfaces are silvered, [m];

θ - angle between normal to the plate surface and incident beam of radiation, [rad].

Infinite summation of the series of reflections gives transmission coefficient T_E of the interferometer as the function of its construction parameters, wavelength of the radiation and direction of the radiation toward interferometer plate [4, 7]:

$$T_E = \frac{(1-R)^2}{1+R^2-R \cdot \cos(\delta)} = \frac{1}{1+F \cdot \sin^2\left(\frac{\delta}{2}\right)} \quad (12)$$

where: R - coefficient of the reflection assumed the same for both surfaces, [-];

F - finesse coefficient of the Fabry-Pérot interferometer:

$$F = \frac{4R}{(1-R)^2} \quad (13)$$

Coefficient of the maximal reflection of the interferometer plate – between spectral windows is given by:

$$R_{\max} = \frac{4 \cdot R}{(1-R)^2} \quad (14)$$

Distance between consecutive spectral windows i.e. peaks of the interferometer characteristics – see Fig. 5, so called **FSR – Free Spectral Range** of the interferometer, which describes the range of unambiguous measurements, is given by the equation:

$$FSR = \Delta\lambda = \frac{\lambda_0^2}{\lambda_0 + 2 \cdot n(\lambda_0) \cdot d \cdot \cos(\theta)} \quad (15)$$

where: λ_0 - wavelength of the peak to whom the FSR is associated when the plate is set appropriately to pass this peak through, [m];

– the rest of variables as in the previous equations.

Shape determination of the peak (transmission window) of the Fabry-Pérot interferometer have to be done at the fixed θ , i.e. for the fixed value of wavelength λ_0 in the center of the peak with

corresponding wave number $k_0 = 2\pi/\lambda_0$ and for the current variable $k = k_s - k_0$ as:

$$\frac{\delta}{2} = (k_s - k_0) \cdot n \cdot d \cdot \cos(\theta) = (k_s - k_0) \cdot c_F \quad (16)$$

where: c_F - coefficient, constant in the contiguity of the peak, [m];

$$c_F = n(\lambda_0) \cdot d \cdot \cos(\theta_0) \quad (17)$$

The relationship between T_E and wave number of the incident radiation should be determined in the nearest vicinity of the peak's center, for the very small values of the δ angle when one can use the approximation $\sin(x) \approx x$:

$$T_E = \frac{1}{1+F \cdot \sin^2((k_s - k_0) \cdot c_F)} \cong \frac{\frac{1}{F \cdot c_F^2}}{\frac{1}{F \cdot c_F^2} + (k_s - k_0)^2} \quad (18)$$

It follows from the equation (18) that the spectral peak placed at the wave number k_0 has the shape described by the curve of the type (3), i.e. Cauchy/Lorentz, where:

$$\gamma = \frac{1}{c_F \cdot \sqrt{F}} \quad (19)$$

The equation (19) allows relating constant γ derived during matching the Voigt profile based function to the Raman spectrum, with technical parameters of the Fabry-Pérot interferometer used as the detector of the scattered radiation. Let make this evaluation for the interferometer which characteristics is depicted on Fig. 5. We have assumed the following construction parameters (realistic!):

- Wavelength of the laser radiation: $\lambda_L = 514$ nm (green-yellowish light);
- Material of the interferometer plate: quartz glass;
- Refraction coefficient of the plate material at laser wavelength: $n = 1.461582$;
- Plate thickness (after tuning of course): $d = 10.5503 \mu\text{m} = 10550.3$ nm;
- Reflection coefficient of the silvered surface: $R = 0.982900$;
- Finesse of the interferometer: $F = 13445.5$;
- Order of the used peak: $m = 30$;
- Free spectral range: $FSR = 8.5295$ nm;
- Parameter γ describing peak shape from equation (19): $\gamma = 5.66 \text{ cm}^{-1}$;
- Extraction of the γ parameter of the Fabry-Pérot interferometer from the Voigt profile matched to the real Raman spectrum from an experiment – investigation of the DLC (Diamond Like Carbon) layer imposed with PVD (Plasma Vacuum Deposition) method on the light alloy, has gave mean value for the all peaks and spectra: $\gamma \approx 5.66 \text{ cm}^{-1}$.

It could be easily seen that matching of the Voigt profile based function has provided us with the very realistic evaluation of the γ parameter. What more this parameter has happen to be at the same level for all the peaks and all the matched spectra. A sample matching result is depicted on the Fig. 6. showing plenty of different carbon forms, which one can expect in the layer. The spread of the γ parameter for all the five matching spectra is exhibited on the Fig. 7.

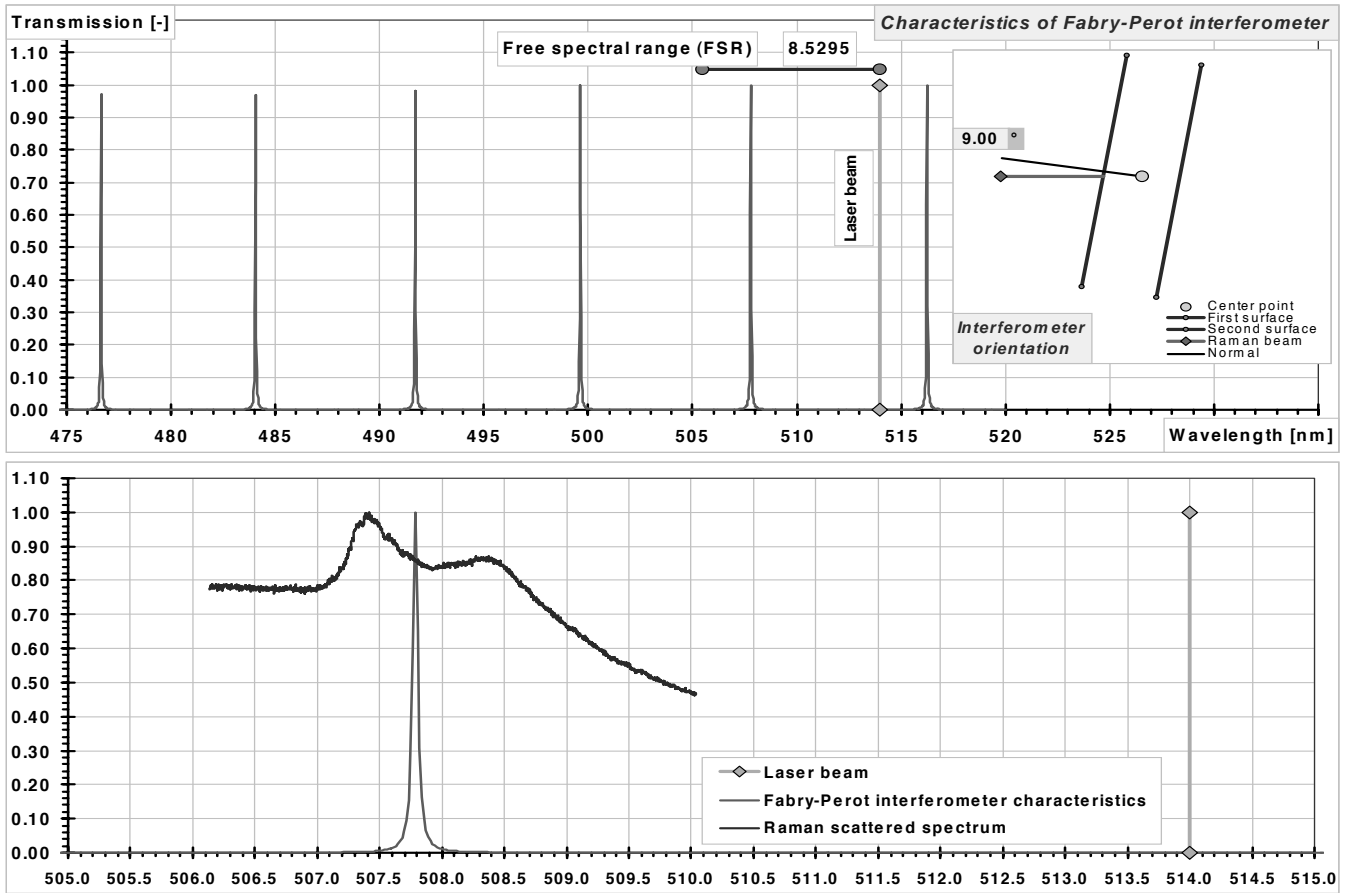


Fig. 5. Simulated characteristics of the Fabry-Pérot interferometer used in the Raman spectrum analyzer. Parameter γ of the interferometer has been extracted from the Voigt profile matched to the Raman spectrum from an experiment, which has been exposed in the background of the lower diagram. The lower diagram is to scale

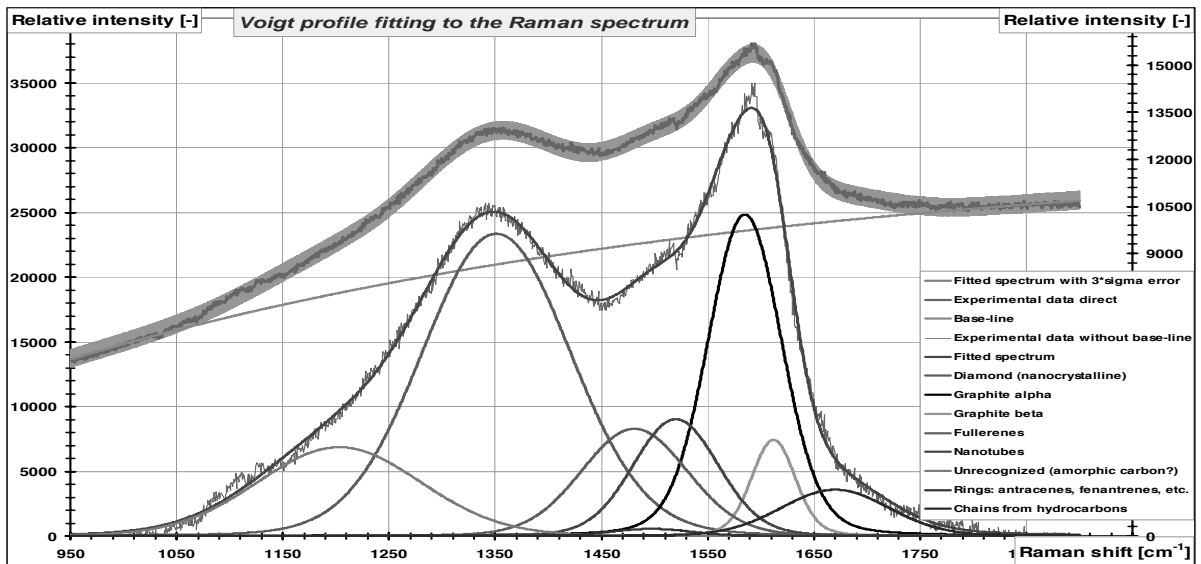


Fig. 6. Matching of the Voigt profile based function to the Raman spectrum of the DLC layer imposed on the light alloy

4. The Voigt profile matching to the Raman spectra

The profile formulas, which could be matched to the Raman spectra, were discussed in details from metrological point of view in our paper [5]. Here we have used Voigt profile based function:

$$I_V(k) = \sum_{n=1}^N I_{0n} \cdot V(k - k_{0n}, \sigma_n, \gamma_n) + (I_{B_{MAX}} - I_{B_{MIN}}) \cdot (1 - \exp(-S_B \cdot k)) + I_{B_{MIN}} \quad (20)$$

where: k_{0n} - wave number of the n -th peak, [m^{-1}];
 I_{0n} - maximal value of the n -th peak, [-];
 σ_n - width of the Gaussian component in the Voigt profile, [m^{-1}];
 γ_n - width of the Cauchy component in the Voigt profile, [m^{-1}].

The proper construction of the base function is a very complicated problem if one would like to relay it upon detailed deliberation about the whole spectrum of the radiation scattered when the laser beam impact sample under test. Here we have made use of a rather simple model, functional not structural, giving baseline of the spectrum (pedestal of the spectrum) as a very "flat" exponential function with three free parameters:

$$I_B(k) = (I_{B_{MAX}} - I_{B_{MIN}}) \cdot (1 - \exp(-S_B \cdot k)) + I_{B_{MIN}} \quad (21)$$

A sight at Fig. 5 with mutual placing of the Raman spectrum and the laser beam allows one to get additional, "visual" justification of the choose expressed in equation (21). Admitting three parameters for baseline function gives sufficient number of degrees of freedom during matching Voigt profile based function (20) to the Raman spectrum. In our case the coefficient S_B was at the level about 0.0009 for all of the analyzed spectra.

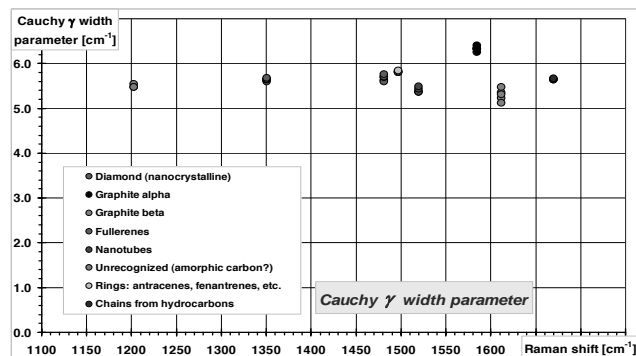


Fig. 7. Distribution of the γ parameter for all the analyzed peaks in the five Raman spectra of the DLC layers

All of the computations related with matching function (20) to the experimental data we have conducted in the calculation diagram built in the *Excel* spreadsheet with application the *Solver* tool. *Solver* seeks for the maximum or minimum of the user-prescribed function in the space of the user-prescribed variables. We have applied the following set-up to the *Solver* tool: searching

for a minimum with using Newton method; scaling at each stage (iteration), square approximation of the function in the minimum vicinity, limit for searching only positive values. The number of variables was in our case as follows:

- 8 peaks with 4 parameters = 32 variables
- baseline function: 3 parameters = 3 variables,
- total: 35 variables.

Results exhibited on Fig. 7. are highly reproducible from peak to peak in the given spectrum and among the Raman spectra obtained from the same spectrometer. It gives an assumption that they truly reflect quality of Fabry-Pérot interferometer and its tuning mode.

5. Conclusions

Accuracy of matching the given Raman spectrum model as Voigt profile with experimental data could be improved basing on some additional information related with Raman spectrometer construction: Fabry-Pérot interferometer quality and its tuning through wavelengths expected in the Raman shift of investigated DLC layer. When performing Raman spectroscopy permanently with the same instrument one can include data related with this instrument, gathered from the previous spectra, in matching process of the current spectrum with Voigt profile.

Investigations described in this paper allow making some assumptions for further research: deconvolution of Raman spectra with Cauchy-type Fabry-Pérot interferometer characteristics. This should give peaks narrowing effect and then, substantial improvement in Raman spectrum recognition due to the material components detection and improvement in quantitative determination of its content.

References

- [1] M. Abramowitz, I.A. Stegun, Handbook of Mathematical Functions, Dover Publications, New York, 1968.
- [2] H.O. Di Rocco, M. Aguirre Téllez, Evaluation of the Asymmetric Voigt Profile and Complex Error Functions in Terms of the Kummer Functions, Acta Physica Polonica 106 (2004) 817-827.
- [3] E. Estevez-Rams, A. Penton, J. Martinez-Garcia, H. Fuess, The use of analytical peak profile functions to fit diffraction data of planar faulted layer crystals, Crystal Research and Technology 40 (2005) 166-176.
- [4] G. Fowles, Introduction to Modern Optics, New York, 1989.
- [5] M. Gołabczak, Protective Carbon Coatings on Magnesium Alloys Manufactured by PACVD Method, Lodz, 2005.
- [6] M. Gołabczak, A. Konstanyowicz, Tools for Quantitative Evaluation of the Raman Spectra of Carbon Layers, Proceedings of 20th European Conference Diamond, Diamond-Like Materials, Carbon Nanotubes and Nitrides DIAMOND2009, Greece, 2009, P2.8.27.
- [7] G. Hernandez, Fabry-Pérot Interferometers, Cambridge, 1986.

- [8] T. Ida, Extended pseudo-Voigt function for approximating the Voigt profile, *Journal of Applied Crystallography* 33 (2000) 1311-1316.
- [9] M. Gołabczak, A. Konstantynowicz, Notices on method of thickness evaluation of the TiN layers on magnesium alloys, *Proceedings of 5th International Conference "Diffusion in Solids and Liquids" DSL2009, Rome, 2009*, 263.
- [10] K.P Reardon, F. Cavallini, Characterization of Fabry-Pérot interferometers and multi-etalon transmission profiles, *Astronomy & Astrophysics* 23 (2008) 897-912.
- [11] J.R. Sandercock, Simple Stabilization Scheme for Maintenance of Mirror Alignment in a Scanning Fabry-Pérot Interferometer, *Journal of Physics* 9 (1976) 566-569.